Achievement of Reactor-Relevant Performance in Negative Triangularity Shape in the DIII-D Tokamak

M. E. Austin, A. Marinoni, M. L. Walker, M. W. Brookman, J. S. deGrassie, A. W. Hyatt, G. R. McKee, C. C. Petty, T. L. Rhodes, S. P. Smith, C. Sung, K. E. Thome, and A. D. Turnbull

Phys. Rev. Lett. **122**, 115001 — Published 18 March 2019

DOI: 10.1103/PhysRevLett.122.115001

Achievement of reactor-relevant performance in negative triangularity shape in the DIII-D tokamak

M.E. Austin,[1,*] A. Marinoni,[2] M.L. Walker,[3] M.W. Brookman,[3] J.S. deGrassie,[3] A.W. Hyatt,[3] G.R. McKee,[4] C.C. Petty,[3] T.L. Rhodes,[5] S.P. Smith,[3] C. Sung,[6] K.E. Thome,[3] and A.D. Turnbull[3]

[1] *The University of Texas at Austin, Austin, TX 78712, USA*
[2] *MIT-Plasma Science and Fusion Center, Cambridge, MA 02139, USA*
[3] *General Atomics, San Diego, CA 92186, USA*
[4] *University of Wisconsin-Madison, Madison, WI 53706, USA*
[5] *University of California-Los Angeles, Los Angeles, CA 90095, USA*
[6] *Lam Research Corp., Fremont, CA 94538, USA*

(Dated: January 22, 2019)

Plasma discharges with negative triangularity ($\delta = -0.4$) shape have been created in the DIII-D tokamak with significant normalized beta ($\beta_N = 2.7$) and confinement characteristic of the high confinement mode ($H_{98y2} = 1.2$) despite the absence of an edge pressure pedestal and no edge localized modes (ELMs). These inner-wall-limited plasmas have similar global performance as a positive triangularity ($\delta = +0.4$) ELMing H-mode discharge with the same plasma current, elongation and cross-sectional area. For cases both of dominant electron cyclotron heating with $T_e/T_i > 1$ and dominant neutral beam injection heating with $T_e/T_i = 1$, turbulent fluctuations over radii $0.5 < \rho < 0.9$ were reduced by 10-50% in the negative triangularity shape compared to the matching positive triangularity shape, depending on radius and conditions.

PACS numbers:

In order for ITER and other future fusion reactors to be successful, the devices must operate with sufficiently long energy confinement times and high plasma pressure. Energy confinement time τ_e is typically defined in terms of global scaling laws extrapolated from data from many devices, and discharges are judged by their confinement scaling factors $H = \tau_e/\tau_e^{\rm scaling}$. Common scalings are H_{89P} [1] and H_{98y2} [2]; good confinement is considered achieved when $H_{89P} > 2$ or $H_{98y2} > 1$. Plasma pressure p is generally described by β, the ratio of p to the pressure exerted by the magnetic field B, $\beta \equiv p/B^2/2\mu_0$. Early studies of tokamaks found an inherent limit to the achievable plasma beta based on magnetohydrodynamic (MHD) stability; the resulting bound is referred to as the Troyon beta limit [3]. This limit depends on the plasma current I, minor radius a and B, hence a normalized beta is often used, $\beta_N = \beta/I/aB$, to allow comparison between different tokamak devices.

To demonstrate high fusion gain, $Q \sim 10$, the ITER reactor will require plasmas with $\beta_N > 1.8$ and $H_{98y2} > 1.0$ [4]. Up to now attainment of these conditions required operation in high-confinement mode or H-mode [5], as opposed to low-confinement mode or L-mode. Values of τ_e are usually a factor of 2 higher in H-mode plasmas, which are characterized by low energy and particle transport at the edge. However, these edge conditions result in high pressures at the periphery that make the discharge susceptible to edge-localized-modes or ELMs [6], which eject energy at levels that could damage reactor walls. Hence much current research is devoted to developing H-modes absent of ELMs, either with regimes that are inherently ELM-free like QH-mode [7] or with ELMs suppressed with edge-resonant magnetic fields [8].

Access to the H-mode regime generally is obtained with sufficient levels of auxiliary heating power and is aided by plasma shaping, with non-circular shapes with a diverted boundary tending to have lower power thresholds for transition. Stretching the plasma vertically and forming a D shape have been found to reduce energy transport and increase the β limit for an MHD instability to cause a disruption [3, 9]. Experiments on TCV showed that creating an *inverse* D, or 'negative triangularity', shape reduced transport even more than the normal D shape and that global confinement could approach H-mode levels [10]. However, those experiments were done with dominant electron cyclotron heating (ECH) and low density, in a regime where the electron temperature T_e exceeded the ion temperature T_i ($T_e/T_i = 2$) and at low plasma beta ($\beta_N = 0.7$). In this Letter, we report on recent experiments in the DIII-D tokamak with a negative triangularity shape and with dominant neutral beam heating (NBI) that led to discharges with $T_e = T_i$, that simultaneously achieved reactor-relevant beta levels and H-mode-level confinement, while maintaining a low edge pressure so as to be inherently ELM-free.

For the experiments in DIII-D [10], a negative triangularity shape was developed within the constraints of the plasma shaping coils and vacuum vessel. A shape with fairly high triangularity, $\delta = -0.4$, with a volume filling 70% of the maximum, was successfully created and is shown in Fig. 1(a). For comparison a matching positive triangularity shape, shown in Fig. 1(b), was created with the same triangularity but opposite sign, and the same elongation ($\kappa = 1.3$) yielding a plasma with the same cross-sectional area. All experiments were done with toroidal field of $B_T = 2.0$ T and plasma current

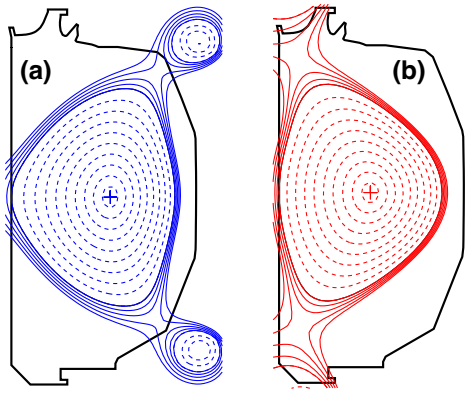

FIG. 1: Cross sections of the DIII-D vessel with flux plots of the (a) negative triangularity ($-\delta$) shape and (b) matching positive triangularity ($+\delta$) shape for the DIII-D experiments with $\delta = \pm 4$ and elongation $\kappa = 1.3$.

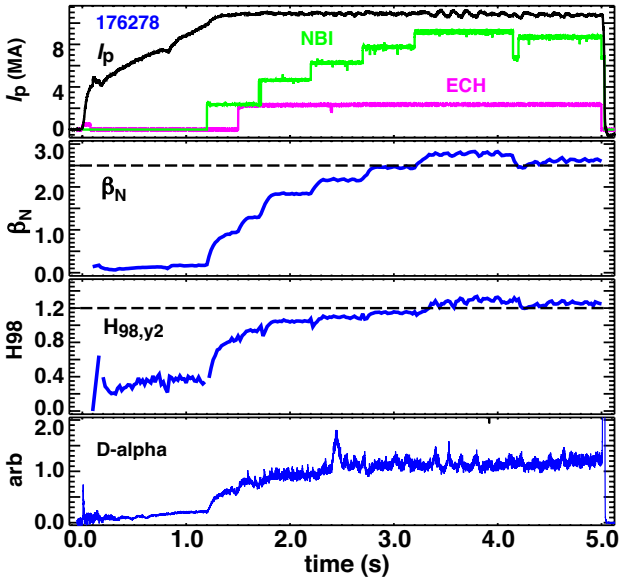

FIG. 2: Time history of a negative triangularity discharge with up to 9.2 MW of NBI and 2.3 MW ECH showing high beta and confinement in the high power phase.

$I_p = 0.9$ MA with plasma major radius $R_0 = 1.7$ m, minor radius $a = 0.59$ m. Due to lower average B_T across the shape, the $-\delta$ discharges had somewhat lower edge safety factor than the $+\delta$, $q_{95} = 3.5$ vs 4.0. Also, due to the geometry, the $-\delta$ discharges have about 9% larger volume, 14 m^{-3} vs 13 m^{-3} for $+\delta$.

The plasmas were heated with up to 10 MW of NBI power and up to 3 MW of ECH power. The discharges were limited on the inner wall of the vessel to mitigate the heat flux that could come through the divertor legs and strike the DIII-D outer wall in regions not adequately shielded to handle the power outflow. Line-averaged density $\overline{n}_e$ ranged from $3.1 - 5.3 \times 10^{19}$ m^{-3} (Greenwald fraction $\overline{n}_e/n_G = 0.38 - 0.64$ where $n_G = I_p/\pi a^2$ is the Greenwald density limit for tokamaks [12].) The dominant impurity was carbon, with typical values of $Z_{\rm eff} \sim 2$.

In the first negative triangularity attempts, the early phase of the discharges were used to investigate the ECH-dominant conditions. The latter half of the discharges were heated with increasing levels of NBI power to look for the threshold for transition to H-mode or the beta limit. Neither was found. Instead, plasmas with confinement factors approaching $H_{98y2} = 1$ and $\beta_N > 2$ were observed, without edge pressure pedestals or ELMs. Subsequently, dedicated $-\delta$ shots with up to 13 MW of combined NBI and ECH were achieved. As shown in a typical shot in Fig. 2, the discharges attained $\beta_N = 2.7$ and $H_{98y2} = 1.2$, sustained for almost 2 s. These discharges were terminated because of energy throughput limitations due to outer-wall-heating concerns or volt-second limits, and not by a disruption. The sustained level of β_N is the highest ever for a DIII-D L-mode discharge.

Experimental operation at elevated beta in negative triangularity plasmas, in the range of ITER operating scenarios ($1.8 < \beta_N < 3.0$), is a surprising result. Historically the $-\delta$ shape has been considered to have low β stability limits to ballooning modes due to the fraction of plasma volume with bad field line curvature. However, a recent study of the $-\delta$ shape found a limit $\beta_N > 3.0$ is possible [13]. Moreover, a study of growth rates of $n = 1$ kink modes using the GATO code [14], employing scaled DIII-D experimental profiles, found a beta limit $\beta_N = 3.1$, so the notion of low β limits in this shape is not borne out in modeling or experiment.

The incremental addition of NBI sources in the negative triangularity discharges, e.g. as depicted in Fig. 2, allowed an examination of the plasma response to increased input power. Figure 3 displays the total stored energy W_{tot} versus total input power P_{tot} calculated from experimental profile data plus ONETWO [15] code runs for ohmic power and fast ion content. The stored energy increases linearly over the range of coupled heating power from 2 to 12 MW.

Shown for comparison is the stored energy expected according to H_{89P} scaling (B_T, I_p, δ, and R_0 were the same for all; $\overline{n}_e$ increased from 3.1 to 5.3×10^{19} m^{-3} over the power scan). Clearly the negative triangularity discharges do not exhibit the degradation in energy confinement typical of L-mode plasmas. Instead, the nearly constant slope indicates the energy confinement time $\tau_E \sim W_{tot}/P_{tot}$ is unvarying with heating power, a feature normally seen only in high performance H-mode discharges [16].

In the experiments comparing matched negative and positive triangularity shapes in the L-mode state, with the same heating power and density, the $-\delta$ discharges outperformed the $+\delta$ ones in terms of stored energy and confinement time. For shots with 3 MW of ECH plus

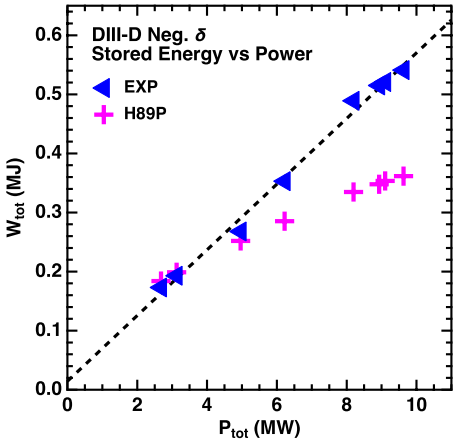

FIG. 3: Total stored energy versus coupled input power for negative triangularity discharges (triangles) and predicted stored energy from H_{89P} scaling (pluses). All discharges had an L-mode edge.

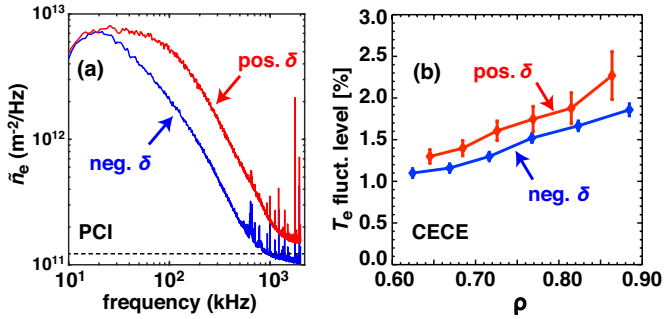

FIG. 4: Comparison of fluctuation levels between matched negative (blue) and positive (red) triangularity shots for (a) PCI diagnostic measuring the spectrum of $\tilde{n}_e$ and (b) CECE diagnostic measuring the T_e fluctuations profile.

10-ms beam blips to obtain T_i and rotation data, central temperatures $T_e \sim 3$ keV and $T_i \sim 1.5$ keV were seen.

In this $T_e > T_i$ case, the negative triangularity discharges had 25% higher stored energy ($W = 0.20$ MJ versus 0.16 MJ) and 26% higher electron energy confinement time ($\tau_E = 88$ ms vs 70 ms) as determined by analysis with ONETWO. Also for these matched discharges, reduced turbulent fluctuation levels were observed in the $-\delta$ shots compared to the $+\delta$.

The magnitude and location of the reduced fluctuations are important for understanding how the improved transport comes about in negative triangularity. In Fig. 4 the two cases are compared with n_e fluctuations measured by the Phase Contrast Imaging (PCI) diagnostic [17] and T_e fluctuations measured with the Correlation ECE (CECE) diagnostic [18]. The PCI system measures line-integrated $\tilde{n}_e$ over a chord that covers $0.4 < \rho < 1.0$, where ρ is the normalized radius (square root of toroidal flux), and k-ranges of $1.5 < k_R < 25$ cm^{-1}, and indicates a $\times 2$ reduction in fluctuation level. The CECE measurement, covering $k_\theta < 1.8$ cm^{-1}, is over six radial locations and shows a reduction of 10-15% in $\widetilde{T}_e$ varying with radius. These results are similar to the reduced fluctuations seen in comparing ohmically heated TCV $+\delta$ and $-\delta$ discharges [19]. However, the DIII-D fluctuation measurements are the first for negative triangularity discharges with substantial NBI heating combined with ECH.

Other comparison discharges were performed with higher matched heating power, obtained by adding up to 7 MW of NBI to the 3 MW of ECH. In these NBI-dominant conditions, the positive triangularity shots went into H-mode while the negative triangularity shots stayed in L-mode, as evidenced by the presence or absence of an edge pedestal and ELMs. Interestingly, both shapes attained nearly the same normalized β, $\beta_N \sim 2.1 - 2.2$ and same H factor, $H_{98y2} = 1.1$, as shown in Fig. 5. Transport analysis from ONETWO indicates that during the high power phase with 10 MW of heating (NBI+ECH), the two discharges had approximately the same stored energy ($W = 0.62$ MJ $-\delta$, 0.60 MJ $+\delta$) and confinement times ($\tau_E = 59$ ms $-\delta$, 58 ms $+\delta$).

Analysis of fluctuation data shows the negative triangularity L-mode discharges had somewhat lower $\tilde{n}_e$ levels than the positive H-mode ones. Figure 6 shows a comparison for the Beam Emission Spectroscopy (BES) diagnostic [20] a 30% reduction for this local measurement at $\rho = 0.7$. PCI data over the same time period indicated a reduction of 50% for this line-averaged measurement.

To identify the turbulent modes active in the DIII-D discharges, linear gyro-kinetic simulations have been carried out with the CGYRO code [21]. They indicate the Trapped Electron Mode (TEM) is the dominant mode in all cases. It is confirmed the TEM are weakened in $-\delta$ compared to the matched $+\delta$ case, as previously shown for low beta, $T_e > T_i$ plasmas [11]. Non-linear gyro-kinetic runs to obtain turbulent heat fluxes are in progress and these along with a comparison with experimental fluxes will be presented in a future publication.

A profile comparison between the matched discharges in the NBI-dominant case shows improved transport for $\rho < 0.95$ in the negative triangularity case makes up for the low edge pedestal. Figure 7 shows profiles of n_e, T_e, T_i, and impurity rotation (carbon) for the two shapes during the time window of 6 MW NBI plus 3 MW ECH. The profiles attain the same central values with $T_e(0) = T_i(0) = 4$ keV with the $+\delta$ shape showing clear edge pedestals indicative of H-mode. The fact that the $-\delta$ discharges, with profiles without a pedestal, attained the same high β_N and H_{98y2} challenges the notion that a pedestal is required for high performance in tokamak discharges.

The results of the first relatively high beta discharges with negative triangularity shaping presented here have significant implications for tokamak energy confinement and future fusion-relevant devices. The improved con-

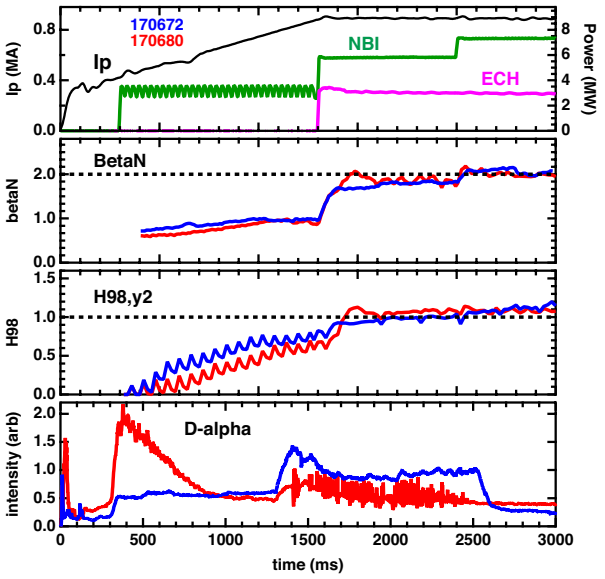

FIG. 5: Time history of matched negative (blue) and positive (red) triangularity discharges with dominant NBI heating. The heating was identical for the two shots up until 2.2 s. The $+\delta$ discharge went into H-mode at 1.4 s; the $-\delta$ discharge retained an L-mode edge throughout.

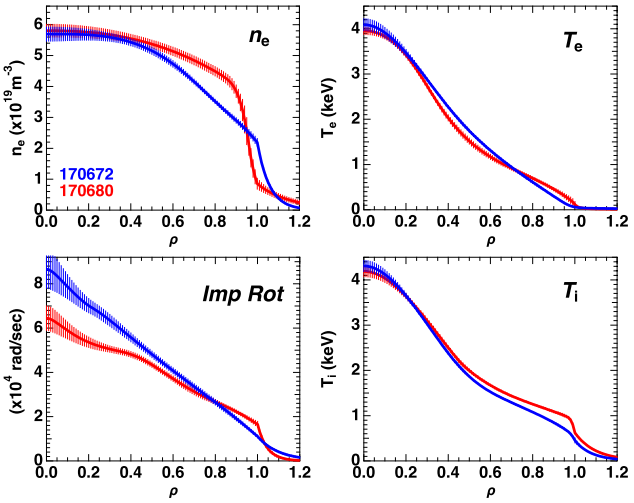

FIG. 7: Profiles of n_e, T_e, T_i and impurity rotation for negative (blue) and positive (red) triangularity discharges. The profiles are an average of 23 time slice fits in the phase 1.5−2.5 s, with constant heating power of 6 MW NBI and 3 MW ECH. Typical data points for one time slice in negative triangularity are shown (gray with error bars).

finement of $-\delta$ due to lower turbulent fluctuation levels, first observed in TCV, has been confirmed in DIII-D for the case of $T_e/T_i > 1$, and demonstrated for the first time for the case $T_e/T_i \sim 1$. The lower turbulence means reduced transport and higher stored energy for given conditions in negative triangularity discharges.

The attainment of high pressure plasmas and H-mode-level confinement, without a pedestal, changes the idea that a fusion reactor has to operate in standard H-mode. One could hope to configure a high-β negative triangularity plasma with unfavorable ion ∇B drift to discourage a transition to H-mode. However, in a $-\delta$ burning plasma there could be sufficient fusion power for an H-mode transition to occur nevertheless. For this case it has been shown in TCV that going from $+\delta$ to $-\delta$ changes the ELMs dramatically —they transition to high-frequency, low-energy types [22] with much lower heat flux to the walls. Either way, running in ELM-free L-mode or with high frequency, low energy ELMs in H-mode, the reactor prospects are better than for conventional $+\delta$ shapes.

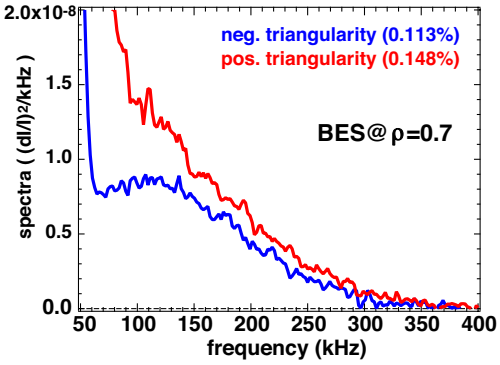

FIG. 6: Comparison of a local measurement of $\tilde{n}_e$ from the BES diagnostic at $\rho = 0.7$ for a negative triangularity L-mode discharge (blue) and a positive triangularity H-mode discharge (red), both with 6 MW of NBI and 3 MW of ECH.

Besides confinement, negative triangularity has other good characteristics for a reactor [23], such as an advantageous position of the divertor at large major radius, providing larger deposition area for heat flux with easier construction. We note that a recent paper reports for one type of plasma shape, that power scrap-off widths decrease by a factor of two when the upper half goes from $+\delta$ to $-\delta$, supposedly reducing the benefits of a negative triangularity shape [24]. However for the shape studied, with an inner wall strike point, the divertor leg displaying narrower heat deposition is relatively short, and the shape in general is far from that expected for a reactor. Overall this identifies the need for more experiments with negative triangularity, with specific configurations relevant to next step fusion devices, e.g. outboard diverted shapes.

The key finding of this work is that a strongly heated negative triangularity shaped tokamak discharge has low energy transport such that even with a low-confinement-type edge it overall has high level energy confinement. Moreover the DIII-D results verify experimentally that the shape is capable of significant, reactor-relevant plasma pressure without disruptive instabilities. This combined with the potential geometric advantages of the shape in terms of heat deposition and construction

economy strongly suggest considering negative triangularity tokamaks for future fusion reactors.

The first author thanks M. Kikuchi for stimulating discussions. This material is based upon work supported by the U.S. Department of Energy, Office of Science, Office of Fusion Energy Sciences, using the DIII-D National Fusion Facility, a DOE Office of Science user facility, under Awards No. DE-FC02-04ER54698, No. DE-AC02-09CH11466, No. DE-AC52-07NA27344, No. DE-FG02-89ER53296, No. DE-FG02-08ER54999, and No. DE-FG02- 95ER54309. DIII-D data shown in this paper can be obtained in digital format by following the links in Ref. [25].

* Electronic address: max.austin@utexas.edu

[1] P. Yushmanov, T. Takizuka, K. Riedel, O. Kardaun, J. Cordey, S. Kaye, and D. Post, Nuclear Fusion **30**, 1999 (1990).

[2] I. P. E. G. on Confinement, Transport, I. P. E. G. on Confinement Modelling, Database, and I. P. B. Editors, Nuclear Fusion **39**, 2175 (1999).

[3] F. Troyon, R. Gruber, H. Sauremann, S. Semenzato, and S. Succi, Plasma Physics and Controlled Fusion **26**, 209 (1984).

[4] M. Shimada, D. Campbell, V. Mukhovatov, M. Fujiwara, N. Kirneva, K. Lackner, M. Nagami, V. Pustovitov, N. Uckan, J. Wesley, et al., Nuclear Fusion **47**, S1 (2007).

[5] F. Wagner, Plasma Physics and Controlled Fusion **49**, B1 (2007).

[6] H. Zohm, Plasma Physics and Controlled Fusion **38**, 105 (1996).

[7] K. H. Burrell, M. E. Austin, D. P. Brennan, J. C. DeBoo, E. J. Doyle, C. Fenzi, C. Fuchs, P. Gohil, C. M. Greenfield, R. J. Groebner, et al., Physics of Plasmas **8**, 2153 (2001).

[8] W. Suttrop, A. Kirk, V. Bobkov, M. Cavedon, M. Dunne, R. McDermott, H. Meyer, R. Nazikian, C. Paz-Soldan, D. Ryan, et al., Nuclear Fusion **58**, 096031 (2018).

[9] P. Angelino, X. Garbet, L. Villard, A. Bottino, S. Jolliet, P. Ghendrih, V. Grandgirard, B. F. McMillan, Y. Sarazin, G. Dif-Pradalier, et al., Physical Review Letters **102**, 195002 (2009).

[10] Y. Camenen, A. Pochelon, R. Behn, A. Bottinoa, A. Bortolon, S. Coda, A. Karpushov, O. Sauter, G. Z. G., and the TCV Team, Nuclear Fusion **47**, 510 (2007).

[11] A. Marinoni, S. Brunner, Y. Camenen, S. Coda, J. P. Graves, X. Lapillonne, A. Pochelon, O. Sauter, L. Villard, and the TCV Team, Plasma Physics and Controlled Fusion **51**, 055016 (2009).

[12] M. Greenwald, Plasma Physics and Controlled Fusion **44**, R27 (2002).

[13] S. Y. Medvedev, M. Kikuchi, L. Villard, T. Takizuka, P. Diamond, H. Zushi, K. Nagasaki, X. Duan, Y. Wu, A. A. Ivanov, et al., Nuclear Fusion **55**, 063013 (2015).

[14] L. C. Bernard, F. J. Helton, and R. W. Moore, Computer Physics Communications **21**, 377 (1981).

[15] H. St John, T. Taylor, Y. Lin-Liu, and A. Turnbull, Plasma Physics and Controlled Nuclear Fusion Research 1994 **3**, 603 (1996).

[16] K. H. Burrell, K. Barada, X. Chen, A. M. Garofalo, R. J. Groebner, C. M. Muscatello, T. H. Osborne, C. C. Petty, T. L. Rhodes, P. B. Snyder, et al., Physics of Plasmas **23**, 056103 (2016).

[17] J. R. Dorris, J. C. Rost, and M. Porkolab, Review of Scientific Instruments **80**, 023503 (2009).

[18] C. Sung, W. A. Peebles, C. Wannberg, L. Rhodes, Terry, X. Nguyen, R. Lantsov, and L. Bardczi, Review of Scientific Instruments **87**, 11E123 (2016).

[19] M. Fontana, L. Porte, S. Coda, O. Sauter, and the TCV Team, Nuclear Fusion **58**, 024002 (2018).

[20] G. McKee, R. Fonck, M. W. Shafer, I. U. Uzun-Kaymak, and Z. Yan, Review of Scientific Instruments **81**, 10D741 (2010).

[21] J. Candy, E. A. Belli, and R. V. Bravenec, Journal of Computational Physics **324**, 73 (2016), ISSN 0021-9991.

[22] A. Pochelon, P. Angelino, R. Behn, S. Brunner, S. Coda, N. Kirneva, S. Y. Medvedev, H. Reimerdes, J. Rossel, O. Sauter, et al., Plasma and Fusion Research **7**, 2502148 (2012).

[23] M. Kikuchi, A. Fasoli, T. Takizuka, P. Diamond, S. Medvedev, X. Duan, H. Zushi, M. Furukawa, Y. Kishimoto, Y. Wu, et al., in *Proc. 1st Int. E-conf. on Energies* (14-31 March 2014), p. E002, www.sciforum.net/conference/ece-1.

[24] M. Faitsch, R. Maurizio, A. Gallo, S. Coda, T. Eich, B. Labit, A. Merle, H. Reimerdes, B. Sieglin, C. Theiler, et al., Plasma Physics and Controlled Fusion **60**, 045010 (2018).

[25] URL https://fusion.gat.com/global/D3D_DMP.